Inactivation of Human MAD2B in Nasopharyngeal Carcinoma Cells Leads to Chemosensitization to DNA-Damaging Agents

Hiu Wing Cheung,[1] Abel C.S. Chun,[2] Qi Wang,[1] Wen Deng,[1] Liang Hu,[3] Xin-Yuan Guan,[3] John M. Nicholls,[4] Ming-Tat Ling,[1] Yong Chuan Wong,[1] Sai Wah Tsao,[1] Dong-Yan Jin,[2] and Xianghong Wang[1]

Departments of [1]Anatomy, [2]Biochemistry, [3]Clinical Oncology, and [4]Pathology, Faculty of Medicine, The University of Hong Kong, Hong Kong, China

Abstract

Rev7p has been suggested to play an important role in regulating DNA damage response in yeast, and recently, the human homologue (i.e., MAD2B) has been identified, which shares significant homology to the mitotic checkpoint protein MAD2. In this study, we investigated whether MAD2B played a key role in cellular sensitivity to DNA-damaging anticancer drugs by suppressing its expression using RNA interference in nasopharyngeal carcinoma cells. Using colony formation assay, we found that suppression of MAD2B conferred hypersensitivity to a range of DNA-damaging agents, especially DNA cross-linkers, such as cisplatin, and γ-irradiation. This effect was associated with reduced frequencies of spontaneous and drug-induced mutations, elevated phosphorylation of histone H2AX, and markedly increased chromosomal aberrations in response to DNA damage. In addition, there was also a significant decrease in cisplatin-induced sister chromatid exchange rate, a marker for homologous recombination-mediated post-replication repair in MAD2B-depleted cells. These results indicate that MAD2B may be a key factor in regulating cellular response to DNA damage in cancer cells. Our findings reveal a novel strategy for cancer therapy, in which cancer cells are sensitized to DNA-damaging anticancer drugs through inactivation of the *MAD2B* gene. (Cancer Res 2006; 66(8): 4357-67)

Introduction

The precise replication of the genome and the maintenance of its integrity are vital for survival and prevention of various diseases, including cancer (1). A family of low fidelity DNA polymerases, such as Pol η, Pol ι, Pol κ, Rev1, and Pol ζ, which mediate translesion DNA synthesis (TLS), are responsible for mutations generated by spontaneous and mutagen-induced DNA damage in yeast (2–4). Studies in yeast showed that Pol ζ consists of two subunits (Rev3p and Rev7p), and Pol ζ activity is estimated to be responsible for at least 60% of spontaneous base substitution mutations in yeast (5, 6). Recent studies using chicken DT40 cells null for Rev3 or Rev7 showed increased chromosomal aberrations, showing that defects in translesion synthesis may cause genomic instability in vertebrate cells (7, 8). Indeed, disruption of Rev3 in mouse was embryonic lethal (9–11), and increased double-strand breaks (DSB) and chromosomal aberrations were also observed in Rev3$^{-/-}$ mouse embryonic cells, supporting the essential role of Pol ζ in maintaining genomic stability in mammalian cells (12). Recently, it was reported that inactivation of Rev3 in cultured human cells by antisense RNA led to reduction of the frequency of UV-induced mutations and increased chemosensitivity to an anticancer drug (cisplatin), suggesting that human Rev3 may have similar functions to its yeast counterpart (13). Although human homologue of yeast Rev7p has been identified, its function is poorly known. Interestingly, its amino acid sequence shares 53% similarity to a key mitotic checkpoint protein mitotic arrest deficient 2 (MAD2); therefore, it is named MAD2-like 2 (MAD2L2) or MAD2B (14, 15). Recently, we found that the MAD2-mediated mitotic checkpoint was essential for DNA damage–induced apoptosis in nasopharyngeal carcinoma cells (16). In addition, evidence of interaction between MAD2B and MAD2 suggests a role of MAD2B in regulating MAD2 stability or activity (15). Therefore, MAD2B has been proposed to function as an adaptor between DNA damage repair and mitotic checkpoint (17).

Several lines of evidence also suggest that human MAD2B and MAD2 have related functions in regulating mitotic checkpoint and the activity of anaphase-promoting complex (APC; ref. 18). *In vitro* studies have shown that the *Xenopus* homologue of MAD2B binds to and inhibits CDC20-APC and CDH1-APC, a ubiquitin ligase controlling chromosome segregation and mitotic exit (19, 20). In addition, in papillary renal cell carcinoma cells, restoration of MAD2B nuclear localization by overexpression of PRCC protein could increase the mitotic checkpoint function in response to nocodazole, a microtubule-disrupting agent (21). Several independent studies based on yeast two-hybrid technology have shown that MAD2B interacts with other proteins, such as adenovirus death protein, trichosanthin, and metalloprotease disintegrin MDC9 (22–24), suggesting that MAD2B might play multiple roles in addition to TLS in the regulation of cell growth.

In this study, we set out to define the roles of MAD2B in human cancer and to investigate if it would be a key regulator of cellular response to chemotherapeutic drugs and DNA-damaging agents in particular. We knocked down the expression of *MAD2B* gene in five nasopharyngeal carcinoma cell lines by RNA interference (RNAi) and studied the cellular sensitivity to a range of anticancer drugs, cellular response to DNA-damaging agents, and mitotic checkpoint control. We found that down-regulation of MAD2B in human nasopharyngeal carcinoma cells conferred hypersensitivity to DNA-damaging anticancer drugs, which was associated with multiple defects in DNA damage tolerance. Our

Note: Supplementary data for this article are available at Cancer Research Online (http://cancerres.aacrjournals.org/).

D-Y. Jin is a Leukemia and Lymphoma Society Scholar.

Requests for reprints: Xianghong Wang, Departments of Anatomy and Biochemistry, The University of Hong Kong, 1/F, Faculty of Medicine Building, 21 Sassoon Road, Hong Kong, China. Phone: 852-2819-2867; Fax: 852-2817-0857; E-mail: xhwang@hkucc.hku.hk or Dong-Yan Jin, E-mail: dyjin@hkucc.hku.hk.

doi:10.1158/0008-5472.CAN-05-3602

results reveal a new strategy to improve the treatment efficiency of DNA-damaging agents through down-regulation of MAD2B expression in cancer cells.

Materials and Methods

Cell culture and transfection. Five nasopharyngeal carcinoma cell lines [CNE1, CNE2 (16), CNE3, HONE1 (25), and TW01 (26)] were maintained in RPMI 1640 (Sigma, St. Louis, MO) supplemented with 2 mmol/L L-glutamine and 5% (v/v) fetal calf serum at 37°C. pLentiviral vector containing short hairpin interfering RNA (shRNA) against MAD2B mRNA (5′-GATGCAGCTTTACGTGGAAGA-3′, 705-725) sequence (pLenti-shMAD2B) was constructed using BLOCK-iT Lentiviral RNAi Expression System (Invitrogen, Carlsbad, CA). Stable transfectants were generated from CNE3, CNE1, CNE2, TW01, and HONE1 cells from a pool of >20 positive clones (which were selected by blasticidin at concentrations of 2, 2.5, 2.5, 4, and 9 μg/mL, respectively). A vector expressing control shRNA sequence (5′-GCGTATTGCCTAGCATTAC-3′), which has no significant homology to any coding sequences in human genome, was used as a vector control. Transfectants were grown for a maximum of 10 passages before retrieving fresh cells from frozen stock, although MAD2B protein levels of cells expressing shMAD2B remained undetectable over 15 passages.

Colony formation assay. Detailed experimental procedures have been described previously (16). Briefly, 500 cells were plated in six-well plates, resulting in 100 to 150 colonies per well after culturing for ~2 weeks. Cisplatin, carboplatin, taxol, mitomycin c (Calbiochem, La Jolla, CA), vincristine, 5-fluorouracil (David Bull Laboratories, Victoria, Australia), chlorethamine, melphalan (Sigma), doxorubicin (EBEWE, Unterach, Austria), or hydrogen peroxide (BDH, Poole, United Kingdom) were added, respectively, 24 hours after plating, and colonies that consisted of >50 cells were scored and compared with the solvent-treated controls. Cells were also γ-irradiated using a γ-Cell 1000 Elite machine at the dose rate of 10 Gy/min. The energy source was ^{137}Cs. Two wells were used for each drug concentration, and five drug concentrations were tested for each experiment. Each experiment was repeated at least thrice, and each survival curve showed the means and SD of at least three independent experiments. Plating efficiency was calculated by counting the number of colonies formed in the control wells divided by number of cells plated then multiplied by 100.

Western blotting. Experiments were carried out as previously described (16). Briefly, cell lysates were prepared by suspending cell pellets in lysis buffer [50 mmol/L Tris-HCl (pH 8), 150 mmol/L NaCl, 1% NP40, 0.5% deoxycholate, and 0.1% SDS], including proteinase inhibitors (1 μg/mL aprotinin, 1 μg/mL leupeptin, and 1 mmol/L phenylmethylsulfonyl fluoride) and phosphatase inhibitors (10 mmol/L sodium fluoride and 5 mmol/L sodium orthovanadate). Protein concentration was measured using D_C Protein Assay kit (Bio-Rad, Hercules, CA). An equal amount of protein (20 μg) was loaded onto an SDS-polyacrylamide gel for electrophoresis and then transferred on a polyvinylidene difluoride membrane (Amersham, Piscataway, NJ). The membrane was then incubated with primary antibodies for 1 hour at room temperature against cyclin B1 (D-11), CDC20 (H-175; 1:500; Santa Cruz Biotechnology, San Diego, CA), MAD2B (1:1,000; Transduction Laboratories, Lexington, KY), CDH1 (DH01; 1:1,000; NeoMarker, Fremont, CA), cleaved caspase-3 (1:500; Cell Signaling Technology, Beverly, MA), or γ-H2AX (Ser^{139}; 1:2,000; Upstate Biotechnology, Lake Placid, NY). After incubation with appropriate secondary antibodies, signals were visualized by enhanced chemiluminescence Western blotting system (Amersham). Expression of actin was also assessed as an internal loading control using a specific antibody (1:2,000; Santa Cruz Biotechnology). Caspase-3 inhibitor Z-DEVD-FMK (Calbiochem) was used at a concentration of 50 μmol/L.

Bromodeoxyuridine incorporation assay. For bromodeoxyuridine (BrdUrd) staining, cells grown on coverslips were treated with 10 μmol/L BrdUrd (Sigma) for 1 hour before fixation in ice-cold 70% ethanol for 20 minutes. Coverslips were rinsed in PBS, incubated in 2 mol/L hydrochloric acid for 20 minutes, and neutralized in 0.1 mol/L borate buffer (pH 8.5) for 5 minutes twice. After blocking in 0.1% bovine serum albumin (BSA) in PBS, cells were incubated with the mouse monoclonal anti-BrdUrd antibody (Roche, Mannheim, Germany). After washing several times in PBS, fluorescein-conjugated goat anti-mouse IgG secondary antibody (1:50) was added for 45 minutes, and the cells were counterstained with 5 μg/mL propidium iodide for 5 minutes. At least 600 cells were counted from three random fields captured by Bio-Rad Radiance 2100 confocal microscopy under ×100 magnification in each experiment, and the percentage of BrdUrd-positive cells was calculated. Each experiment was repeated at least thrice, and error bars indicate the SD of the means.

Immunofluorescent staining of γ-H2AX. CNE1 or HONE1 cells (2×10^4) were plated onto 24-well plates, containing 12-mm coverslips (IWAKI, Tokyo, Japan). Cells were treated with a range of cisplatin doses (0.167, 0.5, and 1.67 μmol/L) or γ-irradiated (1, 2, and 4 Gy) and fixed in 4% paraformaldehyde in PBS at 24 hours after treatment for 10 minutes. Cells were washed thrice in PBS and permeabilized in 0.1% Triton X-100 for 5 minutes. After blocking in 1% BSA in PBS for 20 minutes, cells were incubated with monoclonal anti-phosphorylated(Ser^{139})-H2AX (γ-H2AX) antibody (1:200; Upstate Biotechnology) for 2 hours. Fluorescein-conjugated goat anti-mouse IgG secondary antibody (1:50) was added for 45 minutes. Cellular DNA was counterstained with 4′,6-diamidino-2-phenylindole (DAPI). Fluorescent signals were visualized with a Zeiss Axiophot microscope (Carl Zeiss, Inc., Thornwood, NY) and photographed using Spot RT digital camera and associated software (Diagnostic Instrument, Sterling heights, MI). At least 500 cells were counted from three random fields under ×200 magnification for each experiment, and the percentage of cells containing >10 fluorescent foci was calculated. Each experiment was repeated at least thrice, and the SD of the means was used as error bars. $P < 0.05$ was considered statistically significant as determined by Mann-Whitney U test.

Terminal deoxynucleotidyl transferase–mediated nick-end labeling staining. CNE1 or HONE1 cells (2×10^4) were plated onto 24-well plates, containing 12-mm coverslips (IWAKI). Cells were treated with a range of cisplatin doses (0.167, 0.5, and 1.67 μmol/L) or γ-irradiation (1, 2, and 4 Gy) and fixed in 4% paraformaldehyde in PBS at indicated time points after treatment for 30 minutes. *In situ* cell death detection kit, Fluorescein, was used to detect apoptotic cells according to the manufacturer's instructions (Roche Diagnostics, Indianapolis, IN). At least 500 cells were counted from three random fields under ×100 magnification for each experiment, and the percentage of terminal deoxynucleotidyl transferase–mediated nick-end labeling (TUNEL)–positive cells was calculated. Each experiment was repeated thrice, and the SD of the means was used as error bars. $P < 0.05$ was considered statistically significant as determined by Mann-Whitney U test.

Determination of mitotic index. Detailed experimental procedures were described in our previous studies (27, 28). Briefly, cells were grown on chamber slides and treated with 50 nmol/L nocodazole and collected at every 6 hours post-exposure time for 42 hours. The cells were fixed in cold methanol/acetone (1:1) for 5 minutes and stained with DAPI. The presence of condensed nuclear DNA indicates mitotic cells. To measure the mitotic index (percentage of viable cells arrested in mitosis), at least 500 cells were counted for each experiment using fluorescence microcopy under ×200 magnification, and the data points represent the average results from three independent experiments.

Cell cycle analysis. Nocodazole release experiments was done as described previously (29). CNE1 or HONE1 cells (1.5×10^6) were plated onto 10-cm culture dishes for 24 hours. After treatment with 330 nmol/L nocodazole (Sigma) for 16 hours, mitotic arrested cells were collected by shaking off gently, washed twice in PBS, and released into prewarmed fresh medium. Cells were collected at different time points for flow cytometry and Western blot analysis. Flow cytometric analysis was done on an EPICS profile analyzer and analyzed using the ModFit LT2.0 software (Coulter, Miami, FL) as described previously (16).

Hypoxanthine phosphoribosyltransferase mutation assay. The frequency of cisplatin-induced mutation at hypoxanthine guanine

phosphoribosyl transferase (*HPRT*) locus was measured as described before (13, 30). Briefly, the cells were grown in RPMI containing 1× HAT supplement (100 μmol/L hypoxanthine, 0.4 μmol/L aminopterin, 16 μmol/L thymidine; Life Technologies, Gaithersburg, MD) for 14 days to reduce the number of preexisting 6-thioguanine-resistant and *HPRT*-deficient mutants. To test the cisplatin-induced mutagenesis, HONE1 cells (2×10^6) were grown in 75-cm^2 flasks for 2 days. Cells were exposed to three doses of cisplatin (8.33, 16.67, and 33.33 μmol/L) for 1 hour, washed twice in fresh medium, and cultured for another 14 days. Cells (1×10^5) were replated into each of five 100-mm tissue culture dishes, and 20 μmol/L 6-thioguanine (Sigma) was added 24 hours later. After 14 days, colonies that consisted of >50 cells were scored, and the frequency of 6-thioguanine resistant mutants was calculated from the equation: frequency of 6-thioguanine resistant mutants = a / [$b(5 \times 10^5)$], where a is the number of colonies present in the five 6-thioguanine treated dishes, and b is the cloning efficiency.

To measure the rate of spontaneous generation of 6-thioguanine-resistant mutants, HONE1 cells (1×10^5) were cultured in a 25-cm^2 flask in 5 mL of RPMI and allowed to proliferate for 4 days. The frequencies of 6-thioguanine-resistant mutants were measured as described above. Cells (1×10^5) were subcultured into a new flask and proliferated for 4 days, and the frequency of 6-thioguanine-resistant mutants was measured again. The process was repeated for a total of thrice. Population doubling was calculated from the equation: population doubling = (ln[total number of cells] − ln[number of cells plated × plating efficiency]) / ln2. The rate of spontaneous generation of resistant mutants was the observed frequency of resistant mutants as a function of population doubling. Each experiment was repeated at least thrice, and the SE was used as error bar. $P < 0.05$ was considered statistically significant as determined by Mann-Whitney U test.

Chromosome breakage analysis. To analyze chromosome breakage, cells were treated with a single dose of cisplatin (1.67 μmol/L) or γ-irradiated (1 Gy) and harvested at 12 hours after treatment with colcemid (0.1 μg/mL) added 3 hours before harvest. Metaphase spreading was done as previously described (31). Briefly, harvested cells were incubated in 0.8% (w/v) sodium citrate solution for 15 minutes at 37°C and fixed in 5% (final concentration) methanol/acetic acid (3:1) for 10 minutes at 37°C. The cells were collected by centrifugation and washed five times in methanol/acetic acid (3:1). The cells were dropped onto clean slides and dried in a warm (50°C) water bath. The cells were stained with DAPI in PBS for 5 minutes, washed in PBS thrice, and mounted in DakoCytomation fluorescent mounting medium (DAKO, Glostrup, Denmark). For chromosome aberrations, only breaks in single chromatid arms (chromatid break) were scored. A minimum of 100 metaphases were scored from three independent experiments. The results were expressed as mean number of chromosomal aberrations per metaphase with SE shown.

Sister chromatid exchange analysis. Sister chromatid exchange (SCE) was measured as described previously by a modified fluorescence-plus-Giemsa technique (32). Briefly, 4×10^5 of HONE1 cells were plated in 60-mm culture dishes for 24 hours at about 40% confluence. Cells were then cultured in the presence of 20 μmol/L BrdUrd for 44 hours with 0.1 μg/mL colcemid (Sigma) added 3 hours before harvest. A range of cisplatin doses (0.167, 0.5, and 1.67 μmol/L) were added 12 hours before harvest. Metaphase spreading was done as described above. The cells were stained with 10 μg/mL Hoechst 33342 in Sorensen's solution (pH 6.8) for 15 minutes followed by exposure to "black light" (λ = 365 nm) for 1 hour using Blak-ray UV lamp (UVP, Inc., Upland, CA). The cells were stained with 5% Giemsa in Sorensen's solution (pH 6.8) for 10 minutes, washed in distilled water, and air-dried. A minimum of 100 metaphases were scored blind from each experiment, and three independent experiments were done. The results were expressed as mean number of SCE per metaphase with SE shown.

Results

Inactivation of MAD2B in nasopharyngeal carcinoma cells. To study the function of MAD2B in human cancer cells, we first knocked down the *MAD2B* gene expression in five nasopharyngeal carcinoma cell lines (CNE1, HONE1, CNE3, TW01, and CNE2). As shown in Fig. 1*A*, MAD2B expression was significantly suppressed in all five cell lines stably transfected with a shRNA against *MAD2B*

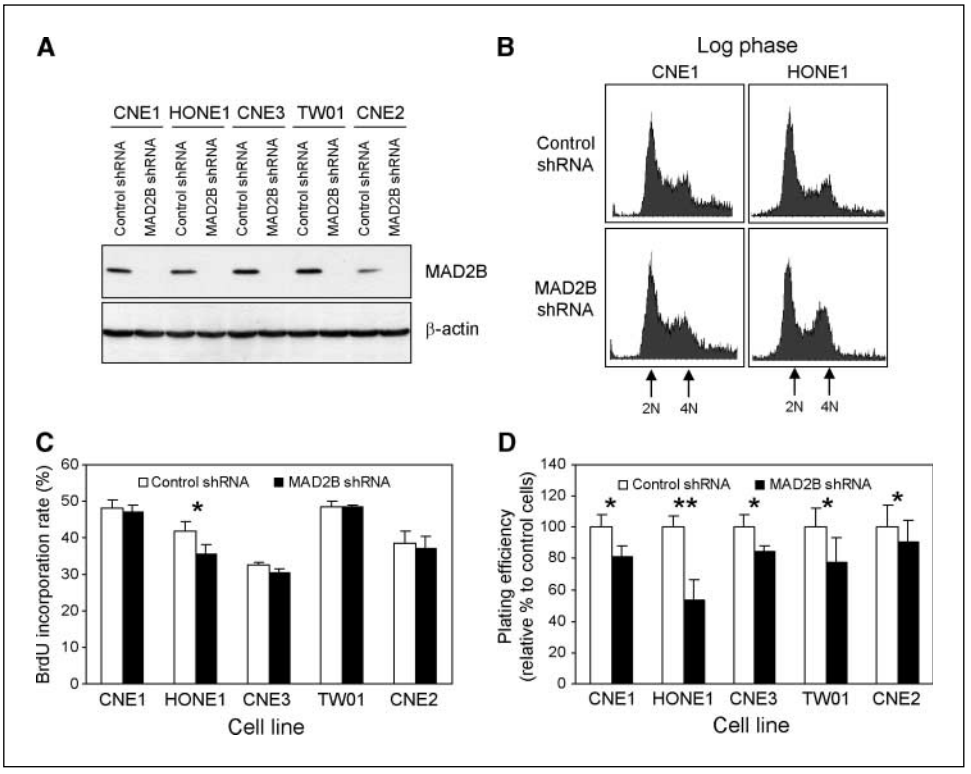

Figure 1. Influence of MAD2B inactivation on cell cycle distribution, proliferation, and plating efficiency in nasopharyngeal carcinoma cell lines. *A,* Western blot analysis of MAD2B expression in five nasopharyngeal carcinoma cell lines (CNE1, HONE1, CNE3, TW01, and CNE2) stably expressing either control shRNA or shMAD2B. Note that transfection of shMAD2B completely abolished MAD2B expression in all five cell lines. *B,* flow cytometric analysis of CNE1 and HONE1 cells expressing control or MAD2B shRNA. *C,* BrdUrd (*BrdU*) incorporation rate between cells expressing control or MAD2B shRNA. *D,* plating efficiency of cells expressing shMAD2B was reduced compared with control cells. *, $P < 0.01$; **, $P < 0.001$.

A

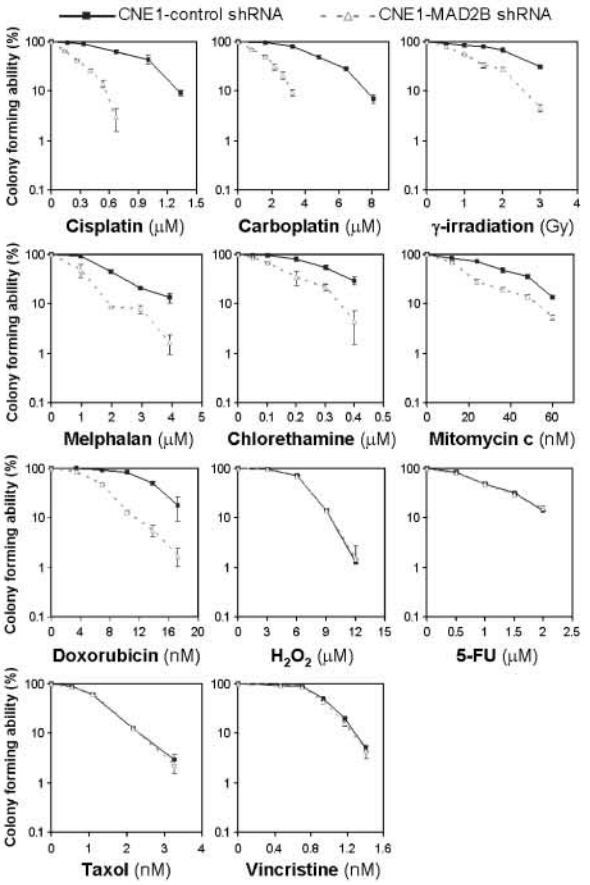

B

Table summarizing the D10 values of the anticancer agents for CNE1 and HONE1 cells expressing control or MAD2B shRNA.

Drugs	CNE1		HONE1	
	Control shRNA (D10)	MAD2B shRNA (D10)	Control shRNA (D10)	MAD2B shRNA (D10)
Cisplatin (μM)	1.33	0.60 *	1.03	0.30 *
Carboplatin (μM)	7.59	3.23 *	6.89	1.56 *
γ-irradiation (Gy)	4.04	2.58 *	3.71	2.1 *
Melphalan (μM)	4.39	2.06 *	3.15	0.69 *
Chlorethamine (μM)	0.46	0.33 *	0.51	0.20 *
Mitomycin c (nM)	66.04	52.37 *	74.69	42.23 *
Doxorubicin (nM)	18.05	10.83 *	21.12	16.00 *
H_2O_2 (μM)	9.21	9.26	8.32	8.12
5-FU (μM)	2.10	2.13	2.71	2.67
Taxol (nM)	2.55	2.59	1.21	1.13
Vincristine (nM)	11.71	11.66	1.77	1.712

D10 = dose that reduces cell survival to 10%, *, $P < 0.01$.

C

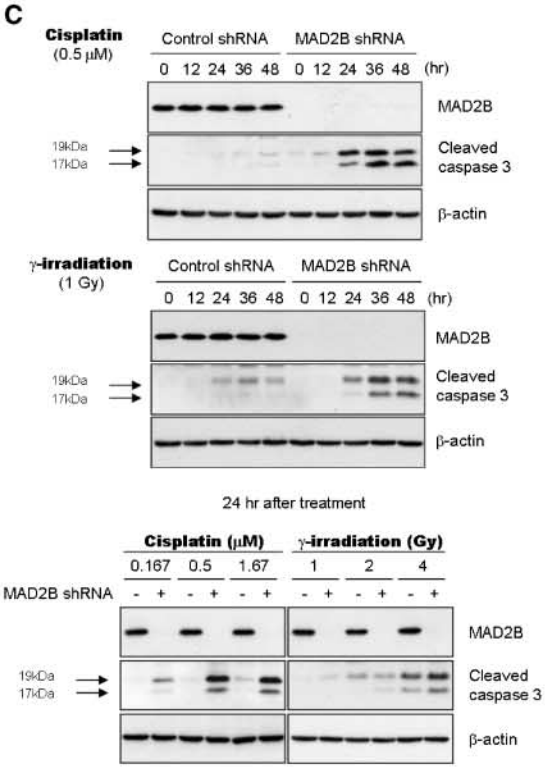

D

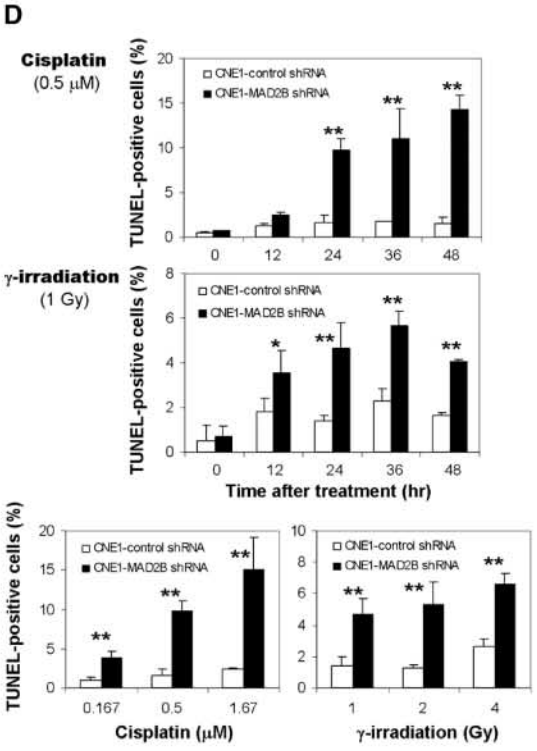

(shMAD2B) compared with the control cells expressing an irrelevant shRNA (control shRNA). Down-regulation of MAD2B did not affect cell cycle distribution as examined by flow cytometry (Fig. 1*B*) or cell proliferation rate as shown by BrdUrd incorporation (Fig. 1*C*), except a small reduction in proliferation rate in HONE1 cells. In contrast, the cells expressing MAD2B shRNA showed significantly reduced plating efficiency (Fig. 1*D*), suggesting that MAD2B deprivation might promote spontaneous apoptosis. These results suggested that silencing of MAD2B expression alone did not have a significant effect on cell cycle distribution or cell proliferation.

MAD2B is required for DNA damage tolerance. In yeast, Rev7p interacts tightly with Rev3p and drastically increases its catalytic activity to synthesize DNA over damaged bases (33). To study if silencing of MAD2B could modulate cellular sensitivity to chemotherapeutic drugs, we examined the clonogenicity of cells with differential MAD2B status in response to genotoxic treatment by colony formation assays. Six types of anticancer drugs were used, including DNA cross-linking agents (cisplatin and carboplatin), DNA-alkylating agents (melphalan, chlorethamine, and mitomycin c), ionizing radiation (γ-rays), topoisomerase II inhibitor (doxorubicin), anti-metabolite (5-fluorouracil), hydrogen peroxide (H_2O_2), and microtubule-disrupting agents (vincristine and taxol). Interestingly, silencing of MAD2B rendered cells generally more sensitive to DNA-damaging agents especially cisplatin and γ-irradiation, as well as melphalan, chlorethamine, and mitomycin c, but not to drugs with different mechanisms of action, such as 5-fluorouracil, hydrogen peroxide, taxol, and vincristine (Fig. 2*A*). Figure 2*B* summarized the D10 values of the anticancer agents for CNE1 and HONE1 cells expressing control or MAD2B shRNA.

To test if the shMAD2B-induced hypersensitivity to DNA-damaging agents was due to activation of apoptotic death, we analyzed the expression of cleaved caspase-3 using Western blotting. After treatment with a relatively low dose of cisplatin or γ-irradiation, a time-dependent increase in the amounts of cleaved caspase-3 was observed in MAD2B-depleted CNE1 cells (Fig. 2*C, top* and *middle*). Similar results were also obtained in the same cells treated with three doses of cisplatin (0.167, 0.5, and 1.67 μmol/L) or γ-irradiation (1, 2, and 4 Gy) for 24 hours (Fig. 2*C, bottom*). To further confirm that shMAD2B sensitized cells to DNA-damaging agents through activation of apoptosis, TUNEL staining was done. Significantly increased number of TUNEL-positive cells was observed in MAD2B-depleted CNE1 cells after treatment with cisplatin or γ-irradiation in a time-dependent and dose-dependent manner (Fig. 2*D*). Thus, inactivation of MAD2B in nasopharyngeal carcinoma cells led to hypersensitivity to certain types of anticancer agents, especially DNA cross-linkers, such as cisplatin, through activation of apoptosis.

Loss of MAD2B reduces mutation rates at *HPRT* locus. In yeast studies, mutants of *Rev* gene family members, such as *Rev1, Rev3*, and *Rev7*, are defective in TLS, leading to reduced mutation rates in response to DNA damage (34). In cultured human fibroblasts, overexpression of antisense RNA targeting Rev1 or Rev3 transcript also results in a reduction in the frequency of UV-induced or cisplatin-induced mutations (13, 35, 36), indicating that the human *Rev* genes may have similar functions to their yeast counterparts. To further understand the molecular mechanism responsible for the shMAD2B-induced chemosensitization, we studied if down-regulation of MAD2B expression had an effect on mutagenic TLS. HPRT assay was done to assess the rates of spontaneous and cisplatin-induced generation of 6-thioguanine-resistant mutants, which reflect the mutation frequencies at the *HPRT* locus (37). Figure 3*A* shows the frequencies of spontaneous generation of 6-thioguanine-resistant mutants were significantly reduced in HONE1 cells expressing low levels of MAD2B compared with those observed in control cells.

To study if MAD2B inactivation also reduced the frequency of DNA damage–induced mutations at the *HPRT* locus, cells were treated with three doses of cisplatin (8.33, 16.67, and 33.33 μmol/L) for 1 hour followed by a 2-week culture, and then the frequencies of 6-thioguanine resistant mutants were measured. The frequencies of 6-thioguanine-resistant mutants induced by cisplatin were significantly reduced in the cells expressing low levels of MAD2B compared with control cells with all doses tested (Fig. 3*B*). That is to say, MAD2B inactivation significantly reduces frequencies of both spontaneous and cisplatin-induced mutations at the *HPRT* locus. These results implicate the importance of human MAD2B for DNA damage tolerance or TLS.

Accumulation of phosphorylated histone H2AX in MAD2B-depleted cells. DSB can be directly produced by ionizing radiation, such as γ-rays (38). Phosphorylation of histone H2AX (γ-H2AX) at Ser^{134} is an early response to DSB that occurs within seconds and could be cytologically visible as "foci" (39, 40). Therefore, analysis of γ-H2AX foci provides one quantitative method to monitor the presence of DSB and the associated repairing activity (41). To investigate if the shMAD2B-induced hypersensitivity to DNA-damaging agents was attributed at least in part to impairment in DNA repair, we did immunofluorescent staining of γ-H2AX. Under untreated condition, silencing of MAD2B resulted in an increase of cells containing >10 γ-H2AX foci compared with control cells (representative photos were shown in Fig. 4*A*, *top* and quantitated in Fig. 4*B*). The difference between the cells with differential MAD2B levels became even more prominent when cells were γ-irradiated at 24 hours time point (Fig. 4*A, middle* and *B*). To further confirm these results, immunoblotting with γ-H2AX antibody was done to compare the relative levels of γ-H2AX after γ-irradiation between cells

Figure 2. Sensitivity of MAD2B-depleted nasopharyngeal carcinoma cells to anticancer drugs. *A,* colony-forming ability of CNE1 cells expressing control or MAD2B shRNA after continuous exposure to various chemotherapeutic drugs with different mechanisms of action. Note that down-regulation of MAD2B conferred hypersensitivity to DNA cross-linking agents (cisplatin and carboplatin), ionizing radiation (γ-rays), alkylating agents (melphalan, chlorethamine, and mitomycin c), and topoisomerase II inhibitor (doxorubicin) but not to 5-fluorouracil, hydrogen peroxide, and microtubule disrupting agents (taxol and vincristine). *Points,* mean of three independent experiments; *bars,* SD. *B,* a table summarizing the D10 values of anticancer agents used against CNE1 and HONE1 cells expressing control or MAD2B shRNA. *, $P < 0.01$. *C,* time-dependent expression of cleaved caspase-3 after exposure to a single dose of cisplatin (0.5 μmol/L, *top*) or γ-irradiation (1 Gy, *middle*) in CNE1 cells. Note that the expression levels of cleaved caspase-3 were significantly higher in the shMAD2B-expressing cells than in control cells in response to the same dose of cisplatin and γ-rays. *Bottom,* dose-dependent expression of cleaved caspase-3 in CNE1 cells expressing control or MAD2B shRNA. Note that the levels of cleaved caspase-3 were significantly higher in shMAD2B-expressing cells in response to three doses of cisplatin or γ-rays. *D,* TUNEL staining of CNE1 cells expressing control or MAD2B shRNA after treatment with cisplatin or γ-irradiation. Note that the number of TUNEL-positive cells was significantly higher in MAD2B-depleted cells after exposure to a single dose of cisplatin (0.5 μmol/L) or γ-irradiation (1 Gy) in a time-dependent manner (*top*) or after exposure to three doses of cisplatin or γ-rays for 24 hours (*bottom*). *Columns,* mean of three independent experiments; *bars,* SD. *, $P < 0.01$; **, $P < 0.001$.

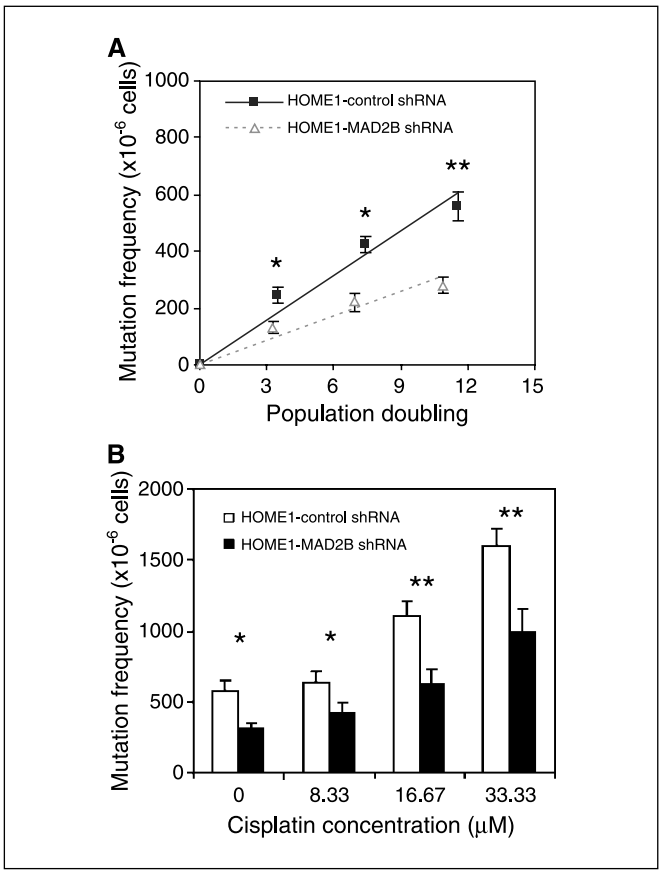

Figure 3. Depletion of MAD2B reduces mutation frequency at the *HPRT* locus. *A,* frequency of spontaneous generation of 6-thioguanine-resistant mutants. Note that HONE1 cells expressing shMAD2B exhibited significantly reduced frequency of 6-thioguanine-resistant mutants compared with cells expressing control shRNA. *B,* frequency of cisplatin-induced generation of 6-thioguanine-resistant mutants. After a 1-hour exposure to three doses of cisplatin (8.33, 16.67, and 33.33 μmol/L) and another 2-week culture, the frequency of 6-thioguanine-resistant mutants was measured. Note that cisplatin-induced generation of 6-thioguanine-resistant mutants was significantly reduced in HONE1 cells expressing shMAD2B compared with control cells in all cisplatin doses tested. *Columns,* mean of three independent experiments; *bars,* SE. *, $P < 0.01$; ** $P < 0.001$.

expressing high and low levels of MAD2B. Consistently, we found that γ-H2AX levels were dramatically increased in cells expressing shMAD2B in both untreated condition and after γ-irradiation (2 Gy) at the 24-hour time point (Fig. 4*C*). To exclude the contribution of apoptotic DNA fragmentation to the γ-H2AX levels, caspase-3 inhibitor (50 μmol/L Z-DEVD-FMK) was added to the cells 1 hour before treatment with cisplatin (0.5 μmol/L) or γ-irradiation (2 Gy), and the γ-H2AX levels were detected at 6 hours after the treatments. At this time point, γ-H2AX levels were also increased in MAD2B-depleted cells compared with control cells (Fig. 4*D*). Thus, down-regulation of MAD2B expression led to an increase in γ-H2AX, indicating that loss of MAD2B resulted in accumulation of DSB in response to endogenous or exogenous DNA damage.

Lack of MAD2B is associated with sister chromatid breaks. Unrepaired DSB is detrimental to cells because it may induce chromosomal aberrations, leading to programmed cell death or tumorigenesis (42). Therefore, next we studied if the MAD2B inactivation-induced chemosensitization was associated with increased chromosomal aberrations. Chromosome spreading was done on HONE1 cells expressing differential levels of MAD2B, and chromosome aberrations were assessed in the untreated and treated cells with a single dose of γ-irradiation (1 Gy) or cisplatin (1.67 μmol/L). It was found that, in untreated condition, a significantly increased amount of single chromatid breaks was observed in cells expressing shMAD2B (shMAD2B: 0.3 ± 0.071 per metaphase versus control shRNA: 0.1 ± 0.043 per metaphase; $P < 0.01$; Fig. 5*B*). The difference was more obvious after treatment with cisplatin (0.82 per metaphase ± 0.13 versus 0.38 ± 0.09 per metaphase; $P < 0.01$; Fig. 5*B, left*) or γ-irradiation (3.94 ± 0.36 per metaphase versus 0.54 ± 0.11 per metaphase; $P < 0.001$; Fig. 5*A* and *B, right*). Thus, the hypersensitivity to DNA damage–induced apoptosis in the cells with low levels of MAD2B is correlated with increased sister chromatid breaks.

Inactivation of MAD2B impairs homologous recombination in response to DNA damage. Studies in chicken cells null for *Rev1, Rev3*, or *Rev7* genes suggest that Rev family proteins participate in homologous recombination–mediated post-replication repair (PRR), which uses intact sister template for repairing DSB (8, 43). In light of this, we investigated the frequency of SCE to assess the homologous recombination events. It was found that in the untreated cells, down-regulation of MAD2B slightly increased the SCE events per cell (Fig. 6*A*, *1* and *2*), and such observation was similar to that observed in chicken DT40 cells null for *Rev3* or *Rev7* (8, 44). After exposure to cisplatin for 12 hours, a marked induction of SCE was observed in the control HONE1 cells (Fig. 6*A*, *1* and *3* and Fig. 6*B*, *top*). In contrast, the induction of SCE by cisplatin was diminished in MAD2B-inactivated HONE1 cells (Fig. 6*A*, *2* and *4* and Fig. 6*B*, *bottom*). The difference was progressively more dramatic as the concentrations of cisplatin were increased (Fig. 6*C*). Hence, inactivation of MAD2B inhibited the induction of SCE in response to DNA damage.

Effect of MAD2B inactivation on mitotic checkpoint. Several studies have shown that in *Xenopus*, MAD2B is able to inhibit APC, the ubiquitin ligase that controls chromosome segregation and mitotic exit through inhibition of its activators CDC20 and CDH1 (18–20). To determine whether down-regulation of MAD2B is influential on mitotic checkpoint control, asynchronous cells expressing control or MAD2B shRNA were treated with nocodazole, a microtubule destabilizer, and mitotic indices were compared. We found that there was no difference in mitotic response between the cells with or without MAD2B protein at six time points tested (Supplementary Fig. S1*A*). In addition, similar percentages of cells undergoing mitotic arrest were observed when five doses of nocodazole were examined (Supplementary Fig. S1*B*). These results were confirmed by flow cytometric analysis (Supplementary Fig. S1*C*), in which no significant difference in the percentage of G_2-M cells was found between the cells with or without MAD2B. Hence, the function of MAD2B in mitotic checkpoint control is very different from that of MAD2 in human cancer cells. To further study the role of MAD2B in mitotic response and to investigate if depletion of MAD2B could cause premature mitotic exit in human cells, the nasopharyngeal carcinoma cells with or without MAD2B were synchronized at mitosis by nocodazole treatment, and the mitotic cells were collected by shake-off, washed, and then replated in fresh medium. Western blot analysis showed that both cell types had similar levels of steady-state cyclin B1 (a substrate of CDC20-APC), CDC20 (a substrate CDH1-APC), and CDH1 (which mediates its own degradation; ref. 45) during mitotic exit (Supplementary Fig. S1*D*; the relative amount of cyclin B1 was shown in

the graphs). Similar results were also obtained in the other three cell lines (data not shown). These data suggested that down-regulation of MAD2B in nasopharyngeal carcinoma cells did not significantly affect the expression and degradation of mitotic regulators.

Discussion

In this study, we provided the first evidence that silencing of MAD2B expression in human nasopharyngeal carcinoma cells led to increased cellular sensitivity to DNA-damaging anticancer drugs. In addition, the shMAD2B-induced hypersensitivity was associated with reduced spontaneous and DNA damage–induced mutagenesis, defective DNA repair, and subsequent activation of apoptosis, suggesting that similar to its yeast counterpart Rev7p, human MAD2B plays an essential role in DNA damage tolerance in cancer cells. Our findings implicate a novel therapeutic target for chemosensitization of human cancer cells.

Roles of MAD2B in TLS. Yeast *Rev7*-null mutant exhibits a reduced rate of mutations induced by DNA-damaging agents (46). In this study, we showed that loss of MAD2B led to reduced rates of spontaneous and cisplatin-induced mutations at the *HPRT* locus (Fig. 3). Consistent with previous findings on human Rev3 and Rev1 (7, 8), this reduction in mutation rates likely reflects a failure in cellular response to DNA damage, which might lead to more dramatic changes, such as chromosomal breaks, thereby causing genome instability. In keeping with this idea, we also showed that down-regulation of MAD2B expression in human nasopharyngeal

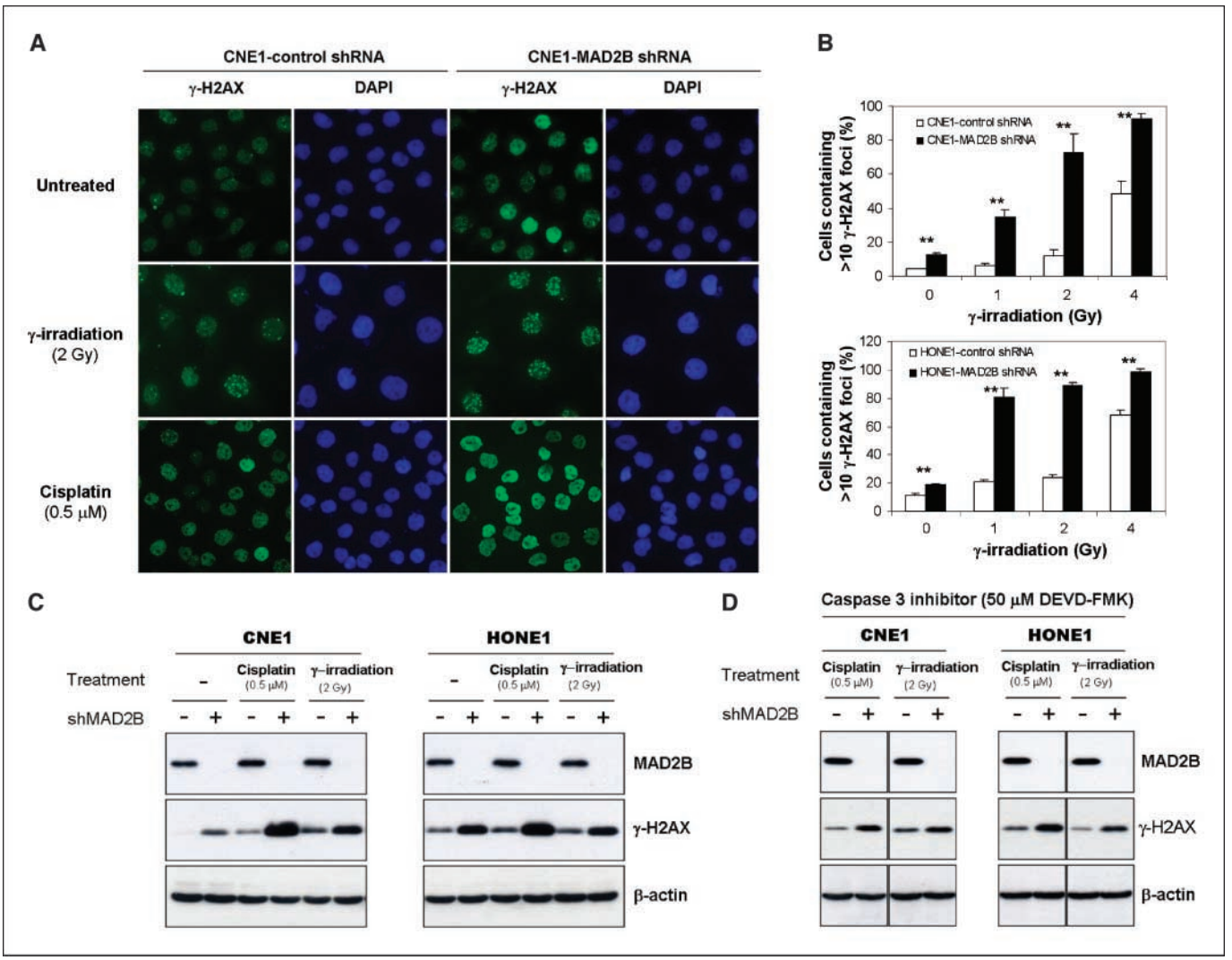

Figure 4. Elevation of γ-H2AX expression level in cells depleted of MAD2B. *A,* immunofluorescent staining of γ-H2AX (*green*) in CNE1 cells expressing control or MAD2B shRNA before treatment (*top*) or 24 hours after treatment with γ-irradiation (2 Gy; *middle*) or cisplatin (0.5 μmol/L; *bottom*). Nuclei were stained with DAPI (*blue*). Images were photographed at the same exposure time under a ×20 objective with a SPOT camera. Note that high % MAD2B shRNA expressing cells showed combination of punctate or homogenous γ-H2AX staining pattern after exposure to γ-rays and cisplatin, respectively. *B,* quantitation of cells containing >10 γ-H2AX foci 24 hours after γ-irradiation treatment. Note that higher percentages of shMAD2B-expressing CNE1 (*top*) and HONE1 (*bottom*) cells showed accumulated γ-H2AX foci compared with control cells. *Columns,* mean of three independent experiments in which 600 cells were counted in each experiment; *bars,* SD. **, $P < 0.001$. *C,* Western blot analysis of γ-H2AX expression after treatment with cisplatin or γ-irradiation in CNE1 and HONE1 cells. Note that the basal level of γ-H2AX was higher in shMAD2B-expressing cells and was increased further in response to cisplatin and γ-irradiation. *D,* Western blot analysis of γ-H2AX expression after treatment with cisplatin or γ-irradiation in the presence of caspase-3 inhibitor. Caspase-3 inhibitor (50 μmol/L Z-DEVD-FMK) was added 1 hour before treatment. Note that the γ-H2AX levels were significantly higher in shMAD2B-expressing cells compared with control cells after treatment for 6 hours.

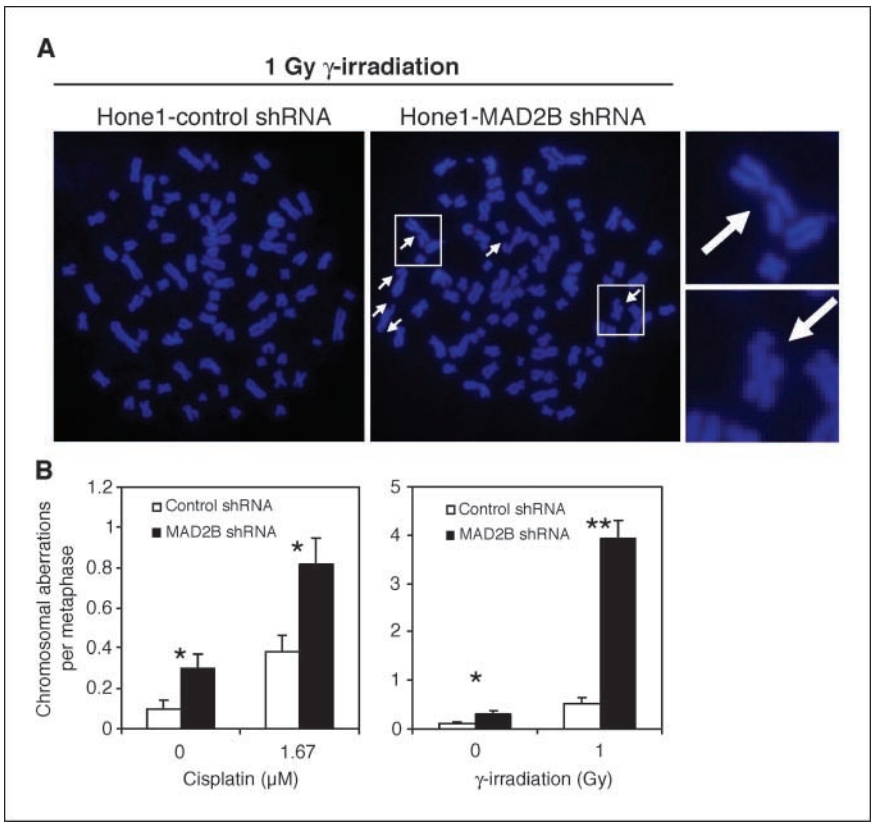

Figure 5. DNA damage–induced chromosomal aberrations in HONE1 cells expressing high or low level of MAD2B. *A,* representative photos of HONE1 cells expressing control or MAD2B shRNA 12 hours after exposure to γ-irradiation (1 Gy). *Arrows,* individual chromosome break. Note that chromosome breaks were significantly more prevalent in shMAD2B expressing cells. *B,* quantitative analysis of chromosomal aberrations of HONE1 cells expressing control or MAD2B shRNA after exposure to cisplatin (1.67 μmol/L; *left*) or γ-irradiation (1 Gy; *right*). *Columns,* mean of three independent experiments in which 100 cells were counted blind; *bars,* SE. *, $P < 0.01$; **, $P < 0.001$.

carcinoma cells conferred hypersensitivity to a wide range of DNA-damaging agents (Fig. 2). This indicates that MAD2B is required for DNA damage tolerance in human cancer cells in a manner similar to its yeast and chicken counterparts. Although we did not have any direct evidence to show that MAD2B directly participates in TLS, previously, it has been shown that MAD2B can undergo homodimerization and form a stable complex with the TLS polymerase subunits Rev1 and Rev3 (15, 47, 48). In addition, MAD2B contains a HORMA domain, which has been suggested to be responsible for protein-protein interaction, oligomerization, and binding to chromatin (49). Furthermore, in the present study, the fact that decreased SCE rate was observed in the MAD2B-depleted cells in response to cisplatin and γ-irradiation (Fig. 6) suggests a role of MAD2B in TLS in human cancer cells. However, the precise role of MAD2B in regulation of TLS as well as how loss of MAD2B affects cellular response to DNA damage merits further investigation.

MAD2B and DNA repair. Repair of DNA DSB, which can be caused by ionizing radiation or DNA cross-linking agents, requires two distinct pathways (i.e., nonhomologous end joining and homologous recombination; ref. 40). We presented several lines of evidence in support of the notion that MAD2B may be critically involved in DNA DSB repair through homologous recombination. First, MAD2B inactivation in nasopharyngeal carcinoma cells caused accumulation of γ-H2AX foci after exposure to γ-rays or cisplatin (Fig. 4). Second, depletion of MAD2B reduced cisplatin-induced SCE (Fig. 6). Finally, loss of MAD2B increased the prevalence of chromosomal breaks (Fig. 5) and increased cellular sensitivity to DNA-damaging agents γ-rays and cisplatin (Fig. 2). Previously, suppression of the expression of the other two *Rev* genes (*Rev1* and *Rev3*) in human cells has also been reported to reduce cisplatin-induced homologous recombination (13, 50), implicating that these error-prone TLS polymerases are also required for PRR mediated by homologous recombination. Consistent with previous findings on Rev1 and Rev3 (7, 8), a reduced rate of DNA damage–induced SCE in MAD2B-depleted cells likely represents a failure in homologous recombination and PRR, which might cause more dramatic changes, such as chromosomal breaks, leading to genome instability.

The molecular mechanisms by which TLS intersects with homologous recombination remain to be understood. Notably, efficient cross-linking and DSB repair require the combined actions of TLS and homologous recombination in chicken DT40 cells (7, 8, 44, 51). However, in response to a base-damaging agent (4-nitroquinoline-1-oxide), increased SCE is seen when TLS is defective (8, 44). This evidence suggests that mammalian cells may preferentially use TLS rather than homologous recombination to response to DNA damage, which has recently been suggested to contribute to loss of heterozygosity (LOH) and genomic instability (52).

MAD2B and mitotic checkpoint control. Previous studies from *Xenopus* and yeast systems suggest that MAD2B plays a role in the regulation of cell cycle progression through the inhibition of CDH1-APC (19–21). In this study, we used RNAi to deplete MAD2B protein in human nasopharyngeal carcinoma cells, whose competency of mitotic checkpoint has been shown to correlate with the level of MAD2 (27). To our surprise, complete knockdown of MAD2B expression in five nasopharyngeal carcinoma cell lines did not affect the rate of cell proliferation, mitotic exit, or competency of mitotic checkpoint (Fig. 1; Supplementary Fig. S1). In stark contrast, reduced expression or disruption of MAD2 results in the loss of mitotic checkpoint (27, 53, 54), suggesting that MAD2B may

play a differential role to MAD2 in mitotic checkpoint control in human cancer cells. Although direct interaction between MAD2 and MAD2B has been reported (15, 17), it is also possible that MAD2 and MAD2B might act independently in regulation of mitotic checkpoint control in certain cell types, such as nasopharyngeal carcinoma cells. It has been shown previously in human papillary renal cell carcinoma cells that expression of PRCC protein enhanced the mitotic checkpoint, probably via restoration of nuclear localization of MAD2B protein (21). Whether the seemingly contradictory observations reflect a cell type–specific function of MAD2B requires further experimentation on additional cell types. Moreover, ectopic expression of green fluorescent protein–tagged MAD2B in the nasopharyngeal carcinoma cells used in this study showed that the majority of MAD2B protein was located in the nucleus (data not shown), and this pattern was different from that in papillary RCC cells where MAD2B was mainly localized in the cytoplasm. It would be of interest to study the differential subcellular localization and activity of MAD2B in various cell lines.

Recently, an alternatively spliced isoform of MAD2 (i.e., MAD2β) has been described in gastric cancer cells (55). Overexpression of MAD2β was found to confer cellular resistance to Adriamycin, which was associated with reduced drug uptake and decreased MAD2 expression. Despite the similar names between MAD2B and MAD2β, they are significantly different in sequence and function (55). Unlike MAD2β, MAD2B modulates neither the expression levels of MAD2 nor the MAD2-induced mitotic checkpoint control in human cancer cells. Because the function of MAD2B or MAD2β is far from clear, further studies are required to elucidate their roles in response to chemotherapeutic drugs.

MAD2B and sensitivity to DNA-damaging anticancer drugs. The *MAD2B* gene is located at the short arm of chromosome 1p36 (14). Interestingly, LOH in this region has been reported in many types of cancers, including nasopharyngeal carcinoma (20-40%; refs. 56, 57), testicular cancer (40%; refs. 58, 59), breast cancer (60%; ref. 60), and neuroblastoma (25%; ref. 61). In addition, decreased *MAD2B* mRNA expression has recently been documented in neuroblastoma compared with normal tissues (62), suggesting that down-regulation of MAD2B may be a frequent event in certain cancers. In the present study, we showed that underexpression or silencing of *MAD2B* drastically increased cellular sensitivity to DNA-damaging agents in nasopharyngeal carcinoma cells (Fig. 2). Based on our analysis, impaired TLS (Fig. 3) or defective PRR mediated through homologous recombination (Fig. 6), which may lead to accumulation of DNA DSBs and activation of apoptosis, could be one explanation for the observed hypersensitivity. Although our results are generally in support of a role for MAD2B in DNA damage response, we can not exclude other possibilities, including the effects on non-DNA targets and/or drug uptake/accumulation. In this connection, additional investigations are

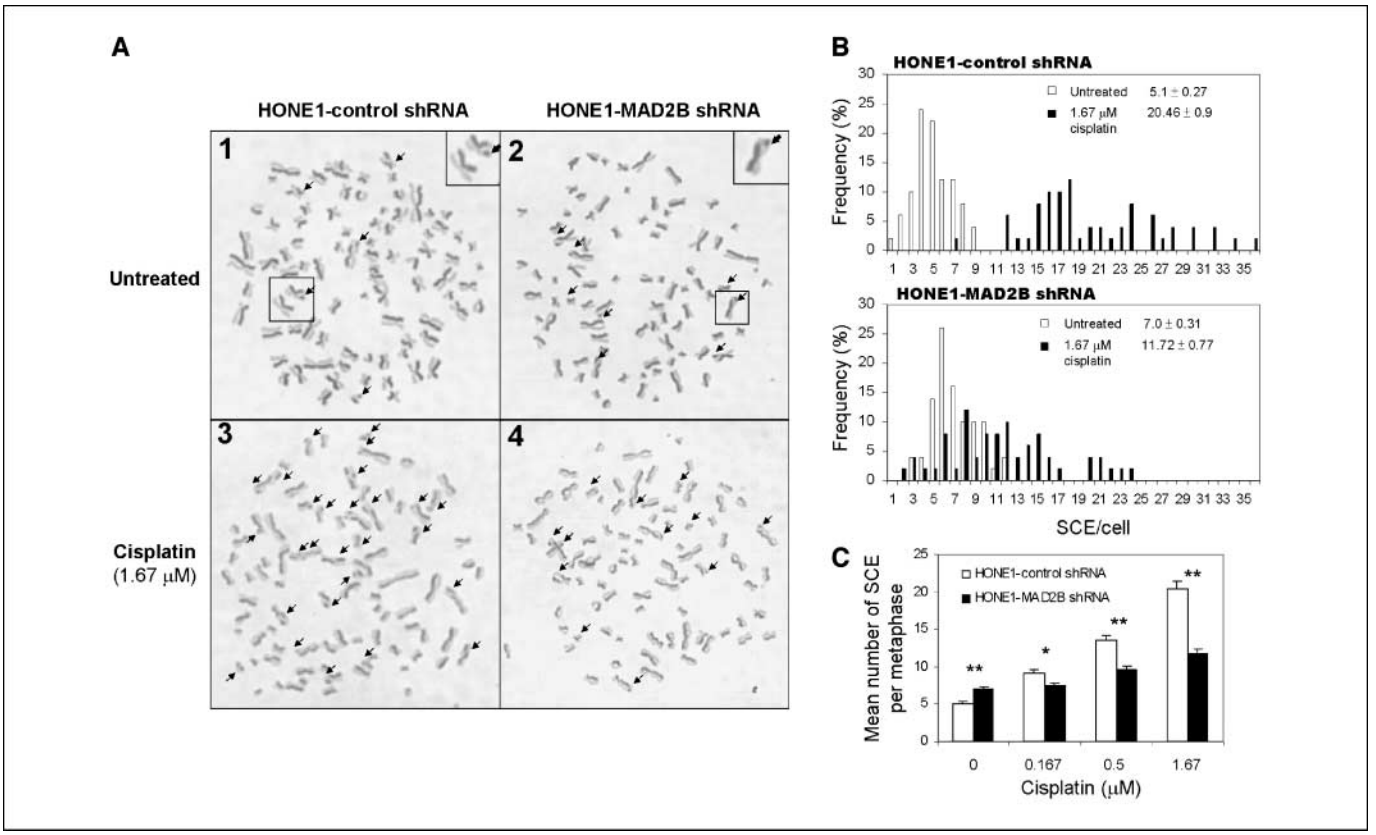

Figure 6. Inactivation of MAD2B attenuates DNA damage–induced SCE. *A,* representative images of SCE metaphases of HONE1 cells expressing control shRNA (*1* and *3*) or shMAD2B (*2* and *4*) before and after exposure to cisplatin (1.67 μmol/L) for 12 hours. *Arrows,* individual SCE events. *B,* distribution of SCE frequency per cell in HONE1 cells expressing control shRNA (*top*) or shMAD2B (*bottom*) before (*open columns*) or after (*solid columns*) treatment with cisplatin (1.67 μmol/L) for 12 hours. Note that the induction of SCE in cells expressing shMAD2B was significantly attenuated. *C,* dose-dependent SCE frequency in HONE1 cells expressing control shRNA or MAD2B shRNA after treatment with a range of cisplatin doses (0.167-1.67 μmol/L) for 12 hours. One hundred metaphases were scored blind in each experiment, and data were generated from three independent experiments and the mean numbers were calculated. *Columns,* mean; *bars,* SE. *, $P < 0.05$; **, $P < 0.001$.

required to elucidate which mechanistic aspects of drug action are truly responsible for the observed sensitization of MAD2B-depleted cells to the subset of chemotherapeutic agents tested in our study. Our results are also supported by a previous study that the LOH at chromosome 1p36 in breast cancer seems to be an indicator for good prognosis (60), suggesting that down-regulation of MAD2B expression might be a biomarker for cellular response to certain chemotherapeutic drugs. Currently, we are examining if decreased MAD2B expression in nasopharyngeal carcinoma patients is correlated with clinical response to radiotherapy and whether it could be used as an indicator to identify potentially responsive patients. On the other hand, our results also indicate that suppression of MAD2B expression in cancer cells might be an alternative strategy to induce chemosensitization. Nevertheless, further analysis based on our findings might lead to the development of a novel strategy to improve treatment efficiencies of certain anticancer drugs.

Acknowledgments

Received 10/6/2005; revised 1/11/2006; accepted 2/10/2006.

Grant support: Hong Kong Research Grants Council grant HKU 7478/03M (X. Wang) and Fogarty International Center of the National Institutes of Health grant D43 TW06186 (D-Y. Jin).

The costs of publication of this article were defrayed in part by the payment of page charges. This article must therefore be hereby marked *advertisement* in accordance with 18 U.S.C. Section 1734 solely to indicate this fact.

We thank Y.P. Ching for stimulating discussions.

References

1. Hoeijmakers JH. Genome maintenance mechanisms for preventing cancer. Nature 2001;411:366–74.
2. Friedberg EC, Gerlach VL. Novel DNA polymerases offer clues to the molecular basis of mutagenesis. Cell 1999;98:413–6.
3. Goodman MF. Error-prone repair DNA polymerases in prokaryotes and eukaryotes. Annu Rev Biochem 2002;71:17–50.
4. Jansen JG, de Wind N. Biological functions of translesion synthesis proteins in vertebrates. DNA Repair (Amst) 2003;2:1075–85.
5. Kunz BA, Ramachandran K, Vonarx EJ. DNA sequence analysis of spontaneous mutagenesis in *Saccharomyces cerevisiae*. Genetics 1998;148:1491–505.
6. Lawrence CW. Cellular roles of DNA polymerase ζ and Rev1 protein. DNA Repair (Amst) 2002;1:425–35.
7. Sonoda E, Okada T, Zhao GY, et al. Multiple roles of Rev3, the catalytic subunit of polζ in maintaining genome stability in vertebrates. EMBO J 2003;22:3188–97.
8. Okada T, Sonoda E, Yoshimura M, et al. Multiple roles of vertebrate REV genes in DNA repair and recombination. Mol Cell Biol 2005;25:6103–11.
9. Bemark M, Khamlichi AA, Davies SL, Neuberger MS. Disruption of mouse polymerase ζ (Rev3) leads to embryonic lethality and impairs blastocyst development *in vitro*. Curr Biol 2000;10:1213–6.
10. Esposito G, Godindagger I, Klein U, Yaspo ML, Cumano A, Rajewsky K. Disruption of the Rev3l-encoded catalytic subunit of polymerase ζ in mice results in early embryonic lethality. Curr Biol 2000;10:1221–4.
11. Wittschieben J, Shivji MK, Lalani E, et al. Disruption of the developmentally regulated *Rev3l* gene causes embryonic lethality. Curr Biol 2000;10:1217–20.
12. Van Sloun PP, Varlet I, Sonneveld E, et al. Involvement of mouse Rev3 in tolerance of endogenous and exogenous DNA damage. Mol Cell Biol 2002;22:2159–69.
13. Wu F, Lin X, Okuda T, Howell SB. DNA polymerase ζ regulates cisplatin cytotoxicity, mutagenicity, and the rate of development of cisplatin resistance. Cancer Res 2004;64:8029–35.
14. Cahill DP, da Costa LT, Carson-Walter EB, Kinzler KW, Vogelstein B, Lengauer C. Characterization of MAD2B and other mitotic spindle checkpoint genes. Genomics 1999;58:181–7.
15. Murakumo Y, Roth T, Ishii H, et al. A human REV7 homolog that interacts with the polymerase ζ catalytic subunit hREV3 and the spindle assembly checkpoint protein hMAD2. J Biol Chem 2000;275:4391–7.
16. Cheung HW, Jin DY, Ling MT, et al. Mitotic arrest deficient 2 expression induces chemosensitization to a DNA-damaging agent, cisplatin, in nasopharyngeal carcinoma cells. Cancer Res 2005;65:1450–8.
17. Murakumo Y. The property of DNA polymerase ζ: REV7 is a putative protein involved in translesion DNA synthesis and cell cycle control. Mutat Res 2002;510:37–44.
18. Vodermaier HC. APC/C and SCF: controlling each other and the cell cycle. Curr Biol 2004;14:R787–96.
19. Chen J, Fang G. MAD2B is an inhibitor of the anaphase-promoting complex. Genes Dev 2001;15:1765–70.
20. Pfleger CM, Salic A, Lee E, Kirschner MW. Inhibition of Cdh1-APC by the MAD2-related protein MAD2L2: a novel mechanism for regulating Cdh1. Genes Dev 2001;15:1759–64.
21. Weterman MA, van Groningen JJ, Tertoolen L, van Kessel AG. Impairment of MAD2B-PRCC interaction in mitotic checkpoint defective t(X;1)-positive renal cell carcinomas. Proc Natl Acad Sci U S A 2001;98:13808–13.
22. Nelson KK, Schlondorff J, Blobel CP. Evidence for an interaction of the metalloprotease-disintegrin tumour necrosis factor alpha convertase (TACE) with mitotic arrest deficient 2 (MAD2), and of the metalloprotease-disintegrin MDC9 with a novel MAD2-related protein, MAD2β. Biochem J 1999;343:673–80.
23. Chan SH, Hung FS, Chan DS, Shaw PC. Trichosanthin interacts with acidic ribosomal proteins P0 and P1 and mitotic checkpoint protein MAD2B. Eur J Biochem 2001;268:2107–12.
24. Ying B, Wold WS. Adenovirus ADP protein (E3–11.6K), which is required for efficient cell lysis and virus release, interacts with human MAD2B. Virology 2003;313:224–34.
25. Glaser R, Zhang HY, Yao KT, et al. Two epithelial tumor cell lines (HNE-1 and HONE-1) latently infected with Epstein-Barr virus that were derived from nasopharyngeal carcinomas. Proc Natl Acad Sci U S A 1989;86:9524–8.
26. Lin CT, Wong CI, Chan WY, et al. Establishment and characterization of two nasopharyngeal carcinoma cell lines. Lab Invest 1990;62:713–24.
27. Wang X, Jin DY, Wong YC, et al. Correlation of defective mitotic checkpoint with aberrantly reduced expression of MAD2 protein in nasopharyngeal carcinoma cells. Carcinogenesis 2000;21:2293–7.
28. Wang X, Jin DY, Ng RW, et al. Significance of MAD2 expression to mitotic checkpoint control in ovarian cancer cells. Cancer Res 2002;62:1662–8.
29. Hsu JY, Reimann JD, Sorensen CS, Lukas J, Jackson PK. E2F-dependent accumulation of hEmi1 regulates S phase entry by inhibiting APC(Cdh1). Nat Cell Biol 2002;4:358–66.
30. Lin X, Ramamurthi K, Mishima M, Kondo A, Christen RD, Howell SB. P53 modulates the effect of loss of DNA mismatch repair on the sensitivity of human colon cancer cells to the cytotoxic and mutagenic effects of cisplatin. Cancer Res 2001;61:1508–16.
31. Deng W, Tsao SW, Lucas JN, Leung CS, Cheung AL. A new method for improving metaphase chromosome spreading. Cytometry A 2003;51:46–51.
32. Spencer T, Butler LJ. A rapid modified fluorescence-plus-Giemsa technique for sister chromatid exchanges and DNA replication patterns. Cytobios 1987;50:145–50.
33. Nelson JR, Lawrence CW, Hinkle DC. Thymine-thymine dimer bypass by yeast DNA polymerase ζ. Science 1996;272:1646–9.
34. Lawrence CW, Maher VM. Mutagenesis in eukaryotes dependent on DNA polymerase ζ and Rev1p. Philos Trans R Soc Lond B Biol Sci 2001;356:41–6.
35. Gibbs PE, McGregor WG, Maher VM, Nisson P, Lawrence CW. A human homolog of the *Saccharomyces cerevisiae* REV3 gene, which encodes the catalytic subunit of DNA polymerase ζ. Proc Natl Acad Sci U S A 1998;95:6876–80.
36. Gibbs PE, Wang XD, Li Z, et al. The function of the human homolog of *Saccharomyces cerevisiae* REV1 is required for mutagenesis induced by UV light. Proc Natl Acad Sci U S A 2000;97:4186–91.
37. Maher VM, McCormick JJ. The *HPRT* gene as a model study for mutation analysis. In: Pfeifer GP, editor. Technologies for detection of DNA damage and mutations. New York: Plenum; 1996. p. 381–90.
38. Karran P. DNA double strand break repair in mammalian cells. Curr Opin Genet Dev 2000;10:144–50.
39. Celeste A, Fernandez-Capetillo O, Kruhlak MJ, et al. Histone H2AX phosphorylation is dispensable for the initial recognition of DNA breaks. Nat Cell Biol 2003;5:675–9.
40. Lisby M, Rothstein R. DNA damage checkpoint and repair centers. Curr Opin Cell Biol 2004;16:328–34.
41. Couedel C, Mills KD, Barchi M, et al. Collaboration of homologous recombination and nonhomologous end-joining factors for the survival and integrity of mice and cells. Genes Dev 2004;18:1293–304.
42. Richardson C, Jasin M. Frequent chromosomal translocations induced by DNA double-strand breaks. Nature 2000;405:697–700.
43. Sonoda E, Takata M, Yamashita YM, Morrison C, Takeda S. Homologous DNA recombination in vertebrate cells. Proc Natl Acad Sci U S A 2001;98:8388–94.
44. Niedzwiedz W, Mosedale G, Johnson M, Ong CY, Pace P, Patel KJ. The Fanconi anaemia gene *FANCC* promotes homologous recombination and error-prone DNA repair. Mol Cell 2004;15:607–20.
45. Listovsky T, Oren YS, Yudkovsky Y, et al. Mammalian Cdh1/Fzr mediates its own degradation. EMBO J 2004;23:1619–26.
46. Baynton K, Bresson-Roy A, Fuchs RP. Distinct roles for Rev1p and Rev7p during translesion synthesis in *Saccharomyces cerevisiae*. Mol Microbiol 1999;34:124–33.
47. Murakumo Y, Ogura Y, Ishii H, et al. Interactions in the error-prone postreplication repair proteins hREV1, hREV3, and hREV7. J Biol Chem 2001;276:35644–51.
48. Masuda Y, Ohmae M, Masuda K, Kamiya K. Structure and enzymatic properties of a stable complex of the human REV1 and REV7 proteins. J Biol Chem 2003;278:12356–60.
49. Aravind L, Koonin EV. The HORMA domain: a common structural denominator in mitotic checkpoints, chromosome synapsis and DNA repair. Trends Biochem Sci 1998;23:284–6.
50. Okuda T, Lin X, Trang J, Howell SB. Suppression of hREV1 expression reduces the rate at which human ovarian carcinoma cells acquire resistance to cisplatin. Mol Pharmacol 2005;67:1852–60.
51. Simpson LJ, Sale JE. Rev1 is essential for DNA damage tolerance and non-templated immunoglobulin gene mutation in a vertebrate cell line. EMBO J 2003;22:1654–64.
52. Luo G, Santoro IM, McDaniel LD, et al. Cancer

predisposition caused by elevated mitotic recombination in Bloom mice. Nat Genet 2000;26:424–9.
53. Burds AA, Lutum AS, Sorger PK. Generating chromosome instability through the simultaneous deletion of *Mad2* and *p53*. Proc Natl Acad Sci U S A 2005;102:11296–301.
54. Michel LS, Liberal V, Chatterjee A, et al. MAD2 haploinsufficiency causes premature anaphase and chromosome instability in mammalian cells. Nature 2001;409:355–9.
55. Yin F, Du Y, Hu W, et al. Mad2β, an alternative variant of Mad2 reducing mitotic arrest and apoptosis induced by Adriamycin in gastric cancer cells. Life Sci 2006;78:1277–86.
56. Lo KW, Teo PM, Hui AB, et al. High resolution allelotype of microdissected primary nasopharyngeal carcinoma. Cancer Res 2000;60:3348–53.
57. Fang Y, Guan X, Guo Y, et al. Analysis of genetic alterations in primary nasopharyngeal carcinoma by comparative genomic hybridization. Genes Chromosomes Cancer 2001;30:254–60.
58. Bussey KJ, Lawce HJ, Himoe E, et al. Chromosomes 1 and 12 abnormalities in pediatric germ cell tumors by interphase fluorescence *in situ* hybridization. Cancer Genet Cytogenet 2001;125:112–8.
59. Summersgill B, Goker H, Weber-Hall S, Huddart R, Horwich A, Shipley J. Molecular cytogenetic analysis of adult testicular germ cell tumours and identification of regions of consensus copy number change. Br J Cancer 1998;77:305–13.
60. Ragnarsson G, Eiriksdottir G, Johannsdottir JT, Jonasson JG, Egilsson V, Ingvarsson S. Loss of heterozygosity at chromosome 1p in different solid human tumours: association with survival. Br J Cancer 1999;79:1468–74.
61. White PS, Thompson PM, Gotoh T, et al. Definition and characterization of a region of 1p36.3 consistently deleted in neuroblastoma. Oncogene 2005;24:2684–94.
62. Janoueix-Lerosey I, Novikov E, Monteiro M, et al. Gene expression profiling of 1p35–36 genes in neuroblastoma. Oncogene 2004;23:5912–22.

Inactivation of Human MAD2B in Nasopharyngeal Carcinoma Cells Leads to Chemosensitization to DNA-Damaging Agents

Hiu Wing Cheung, Abel C.S. Chun, Qi Wang, et al.

Cancer Res 2006;66:4357-4367.